

$\Delta\Delta G_{\text{fit}}^0$. In addition to this, for five of the mutants studied, it was possible to perform an independent check of the $\Delta\Delta G_{\text{fit}}^0$ value obtained by comparing the $\Delta\Delta G_{\text{fit}}^0$ with the relative free energy difference determined from electrochemical measurements of the reaction center ($\Delta\Delta G_{\text{P/P}^+}^0$, Fig. 4 and table S1). In these mutants, only the P/P⁺ midpoint potential (and not the midpoint potentials of B_A/B_A⁻ or H_A/H_A⁻) are thought to change. Therefore, the relative driving force for each of these mutants should be directly related to the measured P/P⁺ midpoint potential via the Nernst equation (26, 27). $\Delta\Delta G_{\text{fit}}^0$ and $\Delta\Delta G_{\text{P/P}^+}^0$ agree to within about 30 meV in all five mutants (Fig. 4), demonstrating that the relative free energies determined from the reaction-diffusion formalism are in line with independently measured values.

These results provide strong experimental evidence for the concept that the complex non-exponential charge separation kinetics in reaction centers largely reflect the time course of protein dynamics rather than the inherent electron transfer rate between two static states. This evidence supports the concept that protein movement plays a key role in the kinetics of the primary electron transfer reaction, as previously modeled in structurally based simulations of electron transfer in reaction centers (14, 15). Apparently, the observed kinetics are determined by protein conformational changes initiated by the light absorption event rather than a static barrier crossing between two potential surfaces. The dependence of electron transfer dynamics on protein movement lends a robustness to the electron transfer process that is likely very advantageous; changes in the local environment that alter the free energy of the charge-separated states (such as membrane potentials, for example) will only have minor effects on the speed and efficiency of the electron transfer reactions, because the protein effectively relaxes through a regime in which the activation energy is nearly zero, almost irrespective of the initial energetics. Given the similarity of the core features of the photosynthetic complexes from bacteria and plants, it is very likely that this same framework holds true for the initial electron transfer reaction of photosynthesis in general and possibly for other protein-mediated electron transfer reactions on similar time scales.

References and Notes

- N. W. Woodbury, J. P. Allen, in *Anoxygenic Photosynthetic Bacteria*, R. E. Blankenship, M. T. Madigan, C. E. Bauer, Eds. (Kluwer, Dordrecht, Netherlands, 1995), vol. 2, pp. 527–557.
- C. Kirmaier, D. Holten, in *The Photosynthetic Reaction Center*, J. Deisenhofer, J. R. Norris, Eds. (Academic Press, San Diego, CA, 1993), pp. 49–70.
- W. Zinth, W. Kaiser, in *The Photosynthetic Reaction Center*, J. Deisenhofer, J. R. Norris, Eds. (Academic Press, San Diego, CA, 1993), pp. 71–88.
- Y. Jia et al., *J. Phys. Chem.* **97**, 13180 (1993).
- P. Huppman et al., *Biophys. J.* **82**, 3186 (2002).
- A. L. M. Haffa et al., *J. Phys. Chem. B* **106**, 7376 (2002).
- M. Du et al., *Proc. Natl. Acad. Sci. U.S.A.* **89**, 8517 (1992).
- P. Hamm et al., *Biochim. Biophys. Acta* **1142**, 99 (1993).
- M. H. Cho, R. J. Silbey, *J. Chem. Phys.* **103**, 595 (1995).
- K. Ando, H. Sumi, *J. Phys. Chem. B* **102**, 10991 (1998).

- W. W. Parson, A. Warshel, *J. Phys. Chem. B* **108**, 10474 (2004).
 - C. Kirmaier, D. Holten, *Proc. Natl. Acad. Sci. U.S.A.* **87**, 3552 (1990).
 - P. D. Laible, S. R. Greenfield, M. R. Wasielewski, D. K. Hanson, R. M. Pearlstein, *Biochemistry* **36**, 8677 (1997).
 - A. Warshel, Z. T. Chu, W. W. Parson, *Science* **246**, 112 (1989).
 - J. N. Gehlen, M. Marchi, D. Chandler, *Science* **263**, 499 (1994).
 - B. H. McMahon, J. D. Muller, C. A. Wraight, G. U. Nienhaus, *Biophys. J.* **74**, 2567 (1998).
 - K. Tomingaga, G. C. Walker, T. J. Kang, P. F. Barbara, T. Fonseca, *J. Phys. Chem.* **95**, 10485 (1991).
 - B. Bagchi, G. R. Fleming, D. W. Oxtoby, *J. Chem. Phys.* **78**, 7375 (1983).
 - H. Sumi, R. A. Marcus, *J. Chem. Phys.* **84**, 4272 (1986); a more complete description of this function as used in the modeling described is given in (20).
 - Materials and methods are available on Science Online.
 - K. Willaert et al., *Biochemistry* **31**, 711 (1992).
 - S. W. Lin, T. P. Sakmar, *Biochemistry* **35**, 11149 (1996).
 - S. Schenkl, F. van Mourik, G. van der Zwan, S. Haacke, M. Chergui, *Science* **309**, 917 (2005).
 - The notation we use for identifying amino acid residues includes the protein subunit letter, the number for the amino acid in the peptide sequence, and the single-letter amino acid abbreviation. Therefore, M185W indicates the Trp at position 185 in subunit M. Single-letter abbreviations for the amino acid residues are as follows: A, Ala; C, Cys; D, Asp; E, Glu; F, Phe; G, Gly; H, His; I, Ile; K, Lys; L, Leu; M, Met; N, Asn; P, Pro; Q, Gln; R, Arg; S, Ser; T, Thr; V, Val; W, Trp; and Y, Tyr. For mutants, we include the original and mutant amino acid. Therefore, L131LH indicates a Leu-to-His mutation at position 131 in subunit L.
 - J. A. Potter et al., *J. Biol. Chem.* **280**, 27155 (2005).
 - X. Lin et al., *Proc. Natl. Acad. Sci. U.S.A.* **91**, 10265 (1994).
 - J. C. Williams, A. L. M. Haffa, J. L. McCulley, N. W. Woodbury, J. P. Allen, *Biochemistry* **40**, 15403 (2001).
 - E. Katilius, J. L. Babendure, S. Lin, N. W. Woodbury, *Photosynth. Res.* **81**, 165 (2004).
 - N. W. Woodbury et al., *Chem. Phys.* **197**, 405 (1995).
 - Figure 3B shows the 280-nm signal from reaction centers that contain quinones. This is because not all of the mutants were stable to quinone removal. As shown in fig. S1, the decay is the same for the first roughly 25 ps, and
- therefore the fact that the decay kinetics on this time scale are identical for all the electron transfer mutants suggests that indeed the time course of protein relaxation is the same for each mutant. This comparison has also been made between wild type and four of the mutants where it was possible to remove quinones without reaction center degradation [M203GL (24), L168HE, L153HS, and L170ND]. All of these kinetic traces are also identical to within the noise of the measurement.
- Besides the electron transfer, another decay path with a time constant of 160 ps is included in the fit, representing the inherent lifetime of P* in the absence of electron transfer. It only affects significantly the kinetics of the double mutants, triple mutant, and L153HD.
 - In Eq. 2, the distinction between ΔG^0 and λ is not very strong. Thus, we report in the text simply the value for the sum. A more complex analysis is required to assign absolute values of these parameters. The value that worked best for ΔG^0 in these fits was –200 meV for wild type, but it is possible to obtain reasonable fits with other values by adjusting λ , although this changes the $\Delta\Delta G_{\text{fit}}^0$ values obtained for the mutants. The ratio of λ_p and λ_t does not vary appreciably with ΔG^0 . In addition, although the reaction-diffusion theory is stated in terms of reorganization occurring on the time scale of electron transfer, it would presumably also be possible to model the system in terms of relaxation of the driving force on the time scale of electron transfer. It should be noted that the exact shape of $C_p(t)$ is not very critical, as explained in the Supporting Online Material (SOM) text.
 - This work was supported by NSF grants MCB0131776, MCB0642260, and MCB0640002. The laser equipment used in this work was purchased with funds from NSF grant BIR9512970. The authors would like to thank E. Katilius for help with the preparation of the L153 mutants and W. Parson, G. Fleming, L. Dutton, N. Hush, S. Boxer, and D. Matyushov for helpful discussions.

Supporting Online Material

www.sciencemag.org/cgi/content/full/316/5825/747/DC1
Materials and Methods
SOM Text
Figs. S1 and S2
Table S1
References

17 January 2007; accepted 16 March 2007
10.1126/science.1140030

Reducing Endogenous Tau Ameliorates Amyloid β -Induced Deficits in an Alzheimer's Disease Mouse Model

Erik D. Roberson,^{1,2*} Kimberly Scarse-Levie,^{1,2} Jorge J. Palop,^{1,2} Fengrong Yan,¹ Irene H. Cheng,^{1,2} Tiffany Wu,¹ Hilary Gerstein,¹ Gui-Qiu Yu,¹ Lennart Mucke^{1,2*}

Many potential treatments for Alzheimer's disease target amyloid- β peptides ($A\beta$), which are widely presumed to cause the disease. The microtubule-associated protein tau is also involved in the disease, but it is unclear whether treatments aimed at tau could block $A\beta$ -induced cognitive impairments. Here, we found that reducing endogenous tau levels prevented behavioral deficits in transgenic mice expressing human amyloid precursor protein, without altering their high $A\beta$ levels. Tau reduction also protected both transgenic and nontransgenic mice against excitotoxicity. Thus, tau reduction can block $A\beta$ - and excitotoxin-induced neuronal dysfunction and may represent an effective strategy for treating Alzheimer's disease and related conditions.

Deposits of amyloid- β peptide ($A\beta$) and tau are the pathological hallmarks of Alzheimer's disease (AD). Treatments aimed at $A\beta$ production, clearance, or aggregation are all in clinical trials. However, interest in

tau as a target has been muted, partly because tau pathology seems to occur downstream of $A\beta$ (1–4), making it uncertain whether tau-directed therapeutics would prevent $A\beta$ -induced impairments. Also, tau is posttranslationally modified in

AD (5–8), and debate continues about which modifications should be targeted. Reducing overall tau levels might be an alternative approach (9). As tau haplotypes driving slightly higher tau expression increase AD risk (10), reducing tau levels might be protective. Therefore, we determined the effect of reducing endogenous tau expression on cognitive deficits in transgenic mice expressing human amyloid precursor protein (hAPP) with familial AD mutations that increase A β production.

We crossed hAPP mice (11) with *Tau*^{-/-} mice (12) and examined hAPP mice with two (hAPP/*Tau*^{+/+}), one (hAPP/*Tau*^{+/-}), or no (hAPP/*Tau*^{-/-}) endogenous tau alleles, compared with *Tau*^{+/+}, *Tau*^{+/-}, and *Tau*^{-/-} mice without hAPP (13). Tau reduction did not affect hippocampal hAPP expression, and conversely, hAPP did not affect hippocampal tau levels (fig. S1). The six genotypes showed no differences in weight, general health, basic reflexes, sensory responses, or gross motor function.

To test learning and memory, we used the Morris water maze. In the cued version, mice learn to find the target platform using a conspicuous marker placed directly above it. At 4 to 7 months of age, *Tau*^{+/+}, *Tau*^{+/-}, and *Tau*^{-/-} mice learned quickly, but as expected (14, 15), hAPP/*Tau*^{+/+} mice took longer to master this task (Fig. 1A; *P* < 0.001). In contrast, hAPP/*Tau*^{+/-} and hAPP/*Tau*^{-/-} mice performed at control levels.

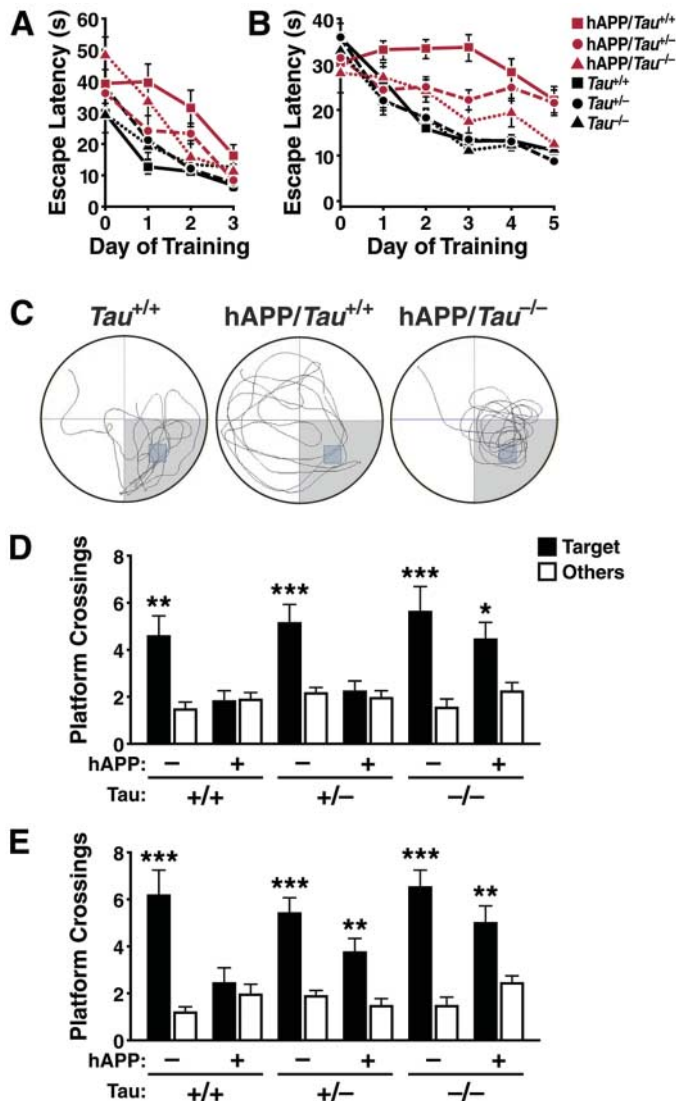
The more difficult hidden-platform version of the water maze demands spatial learning. Mice without hAPP learned this task over 3 days of training regardless of tau genotype, whereas hAPP/*Tau*^{+/+} mice showed no evidence of learning until days 4 and 5 (*P* < 0.001; Fig. 1B). Notably, hAPP/*Tau*^{+/-} mice were less impaired than hAPP/*Tau*^{+/+} mice (*P* < 0.02), and hAPP/*Tau*^{-/-} mice did not differ from controls without hAPP (Fig. 1B). Probe trials, in which the platform was removed and mice were given 1 min to explore the pool, confirmed the beneficial effect of tau reduction (Fig. 1, C to E). In an initial probe trial 24 hours after 3 days of training, hAPP/*Tau*^{+/+} mice had no apparent spatial memory of the platform location, crossing the target platform location no more than they crossed equivalent areas in nontarget quadrants (Fig. 1D). However, hAPP/*Tau*^{+/-} mice, similar to mice without hAPP, did cross the target platform location more often (*P* < 0.01; Fig. 1D). After two additional days of training, hAPP/*Tau*^{+/-} mice also had more target than nontarget crossings (*P* < 0.01), whereas hAPP/*Tau*^{+/+} mice still showed no spatial learning and memory (Fig. 1E). Thus, the tau reduction gene dose-dependently ameliorates A β -dependent water maze learning and memory deficits.

Increased exploratory locomotor activity is seen after entorhinal cortex lesions and may reflect deficits in spatial information processing (16); hAPP mice show similar hyperactivity (15). hAPP/*Tau*^{+/+} mice were hyperactive in the Y maze (*P* < 0.001; Fig. 2A), a new cage (*P* < 0.05; Fig. 2B), and the elevated plus maze (*P* < 0.001; Fig. 2C). In contrast, these abnormalities were not seen in hAPP/*Tau*^{+/-} and hAPP/*Tau*^{-/-} mice (Fig. 2, A to C). To determine whether the benefits afforded by tau reduction were sustained, we examined older mice. Hyperactivity persisted in hAPP/*Tau*^{+/+} mice and remained absent in hAPP/*Tau*^{+/-} mice at 12 to 16 months (*P* < 0.05; Fig. 2D).

Premature death of unclear etiology was also observed in hAPP mice (*P* < 0.005; Fig. 2E) (17, 18). Again, both hAPP/*Tau*^{+/-} and hAPP/*Tau*^{-/-} mice were protected from this early mortality. Thus, tau reduction prevented major A β -dependent adverse effects in hAPP mice. We examined several plausible mechanisms by which tau reduction might exert protective effects and we eventually discovered an unexpected role for tau.

We first ruled out the possibility that tau reduction altered A β levels or aggregation. Tau reduction did not alter hAPP expression (fig. S1), soluble A β _{1-x} or A β ₁₋₄₂ levels, or the A β ₁₋₄₂/A β _{1-x} ratio (fig. S2). In addition, hAPP/*Tau*^{+/+}, hAPP/*Tau*^{+/-}, and hAPP/*Tau*^{-/-} mice had similar plaque load at

Fig. 1. Tau reduction prevented water maze deficits in hAPP mice (*n* = 7 to 11 mice per genotype, age 4 to 7 months). (A) Cued platform learning curves. Day 0 indicates performance on the first trial, and subsequent points represent average of all daily trials. Performance differed by genotype (repeated measures analysis of variance (RMANOVA): *P* < 0.001; hAPP by tau interaction, *P* = 0.058). In post-hoc comparisons, only hAPP/*Tau*^{+/+} differed from groups without hAPP (*P* < 0.001). (B) Hidden platform learning curves differed by genotype (RMANOVA: *P* < 0.001; hAPP by Tau interaction, *P* < 0.02). In post-hoc comparisons, hAPP/*Tau*^{+/+} differed from all groups without hAPP (*P* < 0.001); hAPP/*Tau*^{+/-} differed from hAPP/*Tau*^{+/+} (*P* < 0.02) and groups without hAPP (*P* < 0.01); hAPP/*Tau*^{-/-} differed from hAPP/*Tau*^{+/+} (*P* < 0.001) but not from any group without hAPP. (C and D) Probe trial 24 hours after completion of 3 days of hidden-platform training. (C) Representative path tracings. (D) Number of target platform crossings versus crossings of the equivalent area in the three other quadrants differed by genotype (target crossing by genotype interaction, *P* < 0.001). In post-hoc comparisons, all genotypes except hAPP/*Tau*^{+/+} and hAPP/*Tau*^{+/-} exhibited a preference for the target location over equivalent areas in the other three quadrants (**P* < 0.05; ***P* < 0.01; ****P* < 0.001). (E) Probe trial 72 hours after completion of 5 days of hidden-platform training. Target platform preference differed by genotype (target crossing by genotype interaction, *P* < 0.001; target crossing by hAPP by tau interaction, *P* < 0.05). In post-hoc comparisons, all genotypes except hAPP/*Tau*^{+/+} exhibited a preference for the target location (***P* < 0.01; ****P* < 0.001). Error bars show SEM.



¹Gladstone Institute of Neurological Disease, San Francisco, CA 94158, USA. ²Department of Neurology, University of California, San Francisco, CA 94158, USA.

*To whom correspondence should be addressed. E-mail: eroberson@gladstone.ucsf.edu (E.D.R.); lmucke@gladstone.ucsf.edu (L.M.)

4 to 7 months (fig. S3) and 14 to 18 months (Fig. 3, A and B). We also found no effect of tau reduction on levels of A β *56, a specific A β

assembly linked to memory deficits (19) (fig. S4). Thus, the beneficial effects of reducing tau were observed without detectable changes

in A β burden, suggesting that tau reduction uncouples A β from downstream pathogenic mechanisms.

Next, we looked for abnormal forms of tau that might act as downstream effectors of A β in hAPP/Tau^{+/+} mice. Major AD-related phosphorylation sites in human tau are conserved in murine tau, including those phosphorylated by proline-directed kinases, such as glycogen synthase kinase (GSK)-3 β and cdk5, or by microtubule affinity-regulating kinase (MARK). Changes in murine tau phosphorylation at these sites are easily detected, for example after brief hypothermia (20) (fig. S4). However, in hippocampal homogenates of 4- to 7-month-old hAPP/Tau^{+/+} mice, we did not find changes in tau phosphorylation at proline-directed kinase sites, including Thr¹⁸¹, Ser²⁰², Thr²³¹, and Ser^{396/404}, or at the primary site for MARK, Ser²⁶² (fig. S5). Generation of neurotoxic tau fragments has also been implicated as a mechanism of A β toxicity (21). Tau-deficient primary neurons are resistant to A β -induced degeneration (3, 22), apparently because A β toxicity in vitro involves production of a 17-kD tau fragment (21). We confirmed the presence of a 17-kD tau fragment in lysates of A β -treated primary neurons, but found no abnormal tau proteolysis in hippocampal homogenates from hAPP mice (fig. S6), suggesting that the neuroprotective effects of tau reduction in the two systems are mechanistically different. The relative lack of modified tau also distinguishes our model from transgenic lines overexpressing tau with mutations that cause frontotemporal dementia, but not AD, in humans (2, 4, 23). In our study, reduction of endogenous, wild-type tau protected hAPP mice against A β -dependent cognitive impairments, and this did not involve the elimination of a large pool of tau with typical AD-associated modifications. Our experiments do not rule out the possibility that another type

Fig. 2. Tau reduction prevented behavioral abnormalities and premature mortality in hAPP mice. (A) Total arm entries during a 6-min exploration of the Y maze ($n = 49$ to 58 mice per genotype; age 4 to 7 months; ANOVA: genotype effect, $P < 0.0001$; hAPP by tau interaction, $P < 0.0001$; *** $P < 0.001$ versus groups without hAPP). (B) Percentage of time spent active during a 5-min exploration of a new cage ($n = 7$ to 14 mice per genotype; age 4 to 7 months; ANOVA: genotype effect, $P < 0.01$; hAPP by tau interaction, $P < 0.05$; * $P < 0.05$ versus groups without hAPP). (C) Total distance traveled in both open and closed arms during a 10-min exploration of the elevated plus maze ($n = 49$ to 59 mice per genotype; age 4 to 7 months; ANOVA: genotype effect, $P < 0.0001$; hAPP by tau interaction, $P < 0.05$; *** $P < 0.001$ versus groups without hAPP). (D) Total distance traveled during exploration of elevated plus maze ($n = 6$ to 13 mice per genotype; age 12 to 16 months; ANOVA: hAPP effect, $P < 0.01$; hAPP by tau interaction, $P = 0.079$; * $P < 0.05$ versus groups without hAPP). Error bars in (A) to (D) show SEM. (E) Kaplan-Meier survival curves showing effect of tau reduction on premature mortality in hAPP mice. All genotyped mice in the colony ($n = 887$) were included in the analysis. By log-rank comparison, only hAPP/Tau^{+/+} mice differed from all other groups ($P < 0.005$).

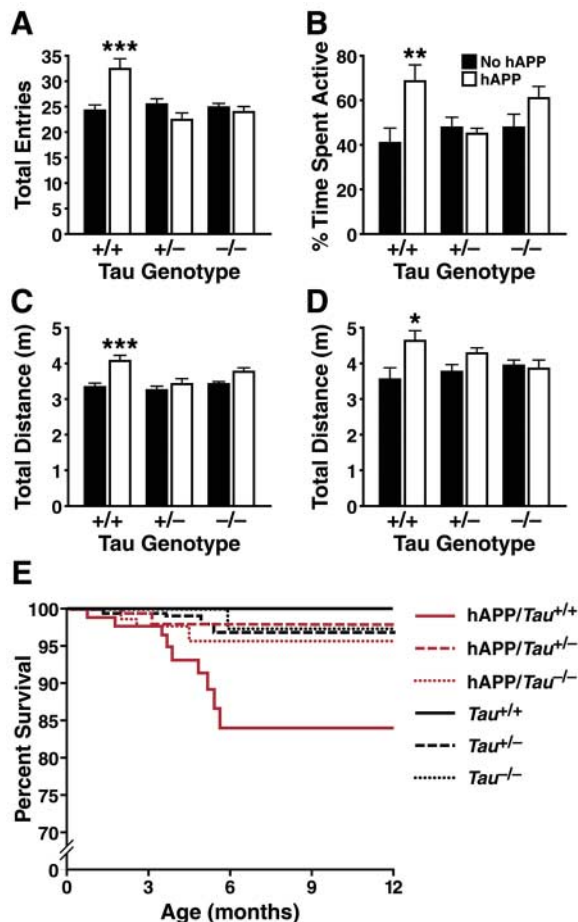
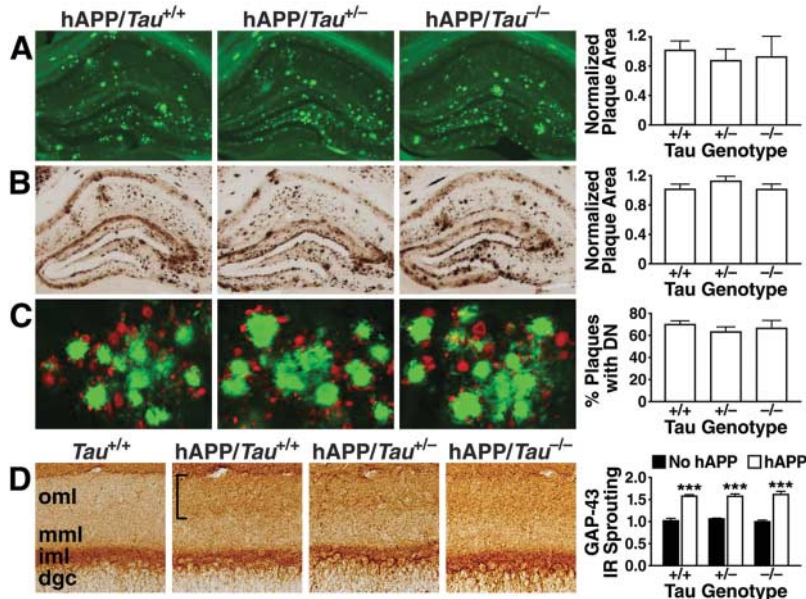


Fig. 3. Tau reduction did not change A β plaque deposition, neurotic dystrophy, or aberrant sprouting. (A) Thioflavin-S staining of hippocampal amyloid plaques in hAPP mice. Percentage of hippocampal area covered by plaques was normalized to the mean value in hAPP/Tau^{+/+} mice ($n = 6$ to 11 mice per genotype; age 14 to 18 months). (B) Immunostaining of hippocampal A β deposits in hAPP mice. Percentage of hippocampal area covered by plaques was normalized to the mean value in hAPP/Tau^{+/+} mice ($n = 6$ to 11 mice per genotype; age 14 to 18 months). (C) Double-labeling of hippocampus for dystrophic neurites (antibody 8E5, red) and amyloid plaques (thioflavin-S, green) in hAPP mice aged 14 to 18 months, with quantification of dystrophic neurites expressed as percentage of thioflavin-S-positive plaques with surrounding neurotic dystrophy ($n = 9$ to 11 mice per genotype). (D) GAP43 immunostaining of aberrant axonal sprouting in the molecular layer of the dentate gyrus (oml, outer molecular layer; mml, middle molecular layer; iml, inner molecular layer; dgc, dentate granule cells). Bracket highlights GAP43-positive sprouting in the outer molecular layer of hAPP mice. Sprouting was quantified by densitometry and normalized to the mean value in Tau^{+/+} mice ($n = 7$ to 14 mice per genotype; age 4 to 7 months; *** $P < 0.001$ versus groups without hAPP). Error bars show SEM.



of tau modification, or a small pool of modified tau in a restricted subcellular compartment or cellular population, could play a role downstream of A β .

To begin addressing this possibility, we stained brain sections from *Tau*^{+/+} and hAPP/*Tau*^{+/+} mice with phospho-tau antibodies. We saw little difference overall between *Tau*^{+/+} and hAPP/*Tau*^{+/+} mice in phospho-tau immunoreactivity, but we did observe scattered phospho-tau-positive punctae in dystrophic neurites surrounding amyloid plaques (fig. S7). We thus wondered whether the benefits of tau reduction in hAPP mice could relate to prevention of neuritic dystrophy, which may contribute to AD-related cognitive decline (24). Despite the differences in their behavior, hAPP/*Tau*^{+/+}, hAPP/*Tau*^{+/-}, and hAPP/*Tau*^{-/-} mice had similar amounts of neuritic dystrophy (Fig. 3C). Thus, tau is not required for the formation of plaque-associated dystrophic neurites. Given that tau reduction prevented behavioral deficits but not neuritic dystrophy, these may represent parallel, rather than causally linked, disease manifestations, or tau reduction may act downstream of neuritic dystrophy.

Tau has a well-characterized role in axonal outgrowth (12), so we tested whether tau reduction prevented the aberrant sprouting of hippocampal axons observed in AD (25) and hAPP mice (18). Similar degrees of sprouting were observed, regardless of tau genotype (Fig. 3D). Thus, although tau reduction affected important outcome measures related to A β -induced neuronal dysfunction, not all effects of A β were blocked.

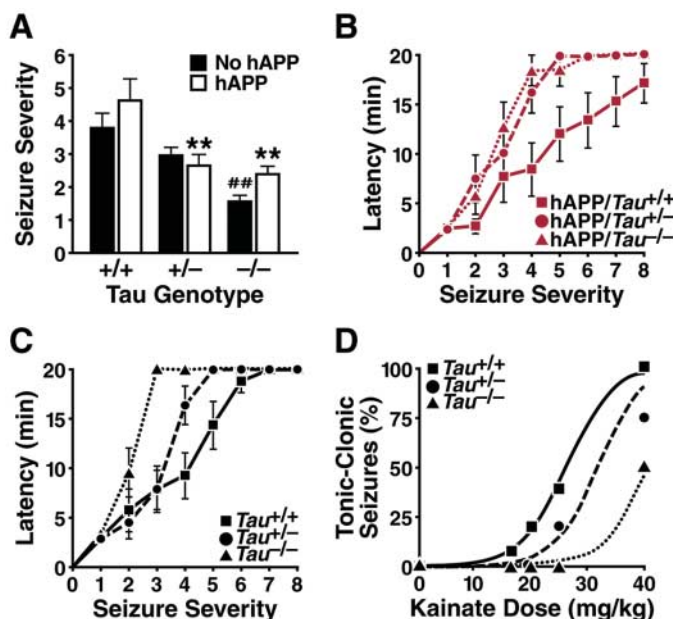
Excitotoxicity is implicated in the pathogenesis of AD (26, 27). Consistent with the increased incidence of seizures in AD patients (28), TgCRND8 hAPP mice are more susceptible to the γ -aminobutyric acid type A (GABA_A) receptor antagonist pentylentetrazole (PTZ) (29). Using a similar paradigm, we found that hAPP/*Tau*^{+/+} mice were also abnormally sensitive to PTZ, with 20% suffering fatal status epilepticus at a dose that was not lethal to mice without hAPP ($P < 0.05$). Tau reduction prevented this effect, as no hAPP/*Tau*^{+/-} or hAPP/*Tau*^{-/-} mice died. Seizures in hAPP/*Tau*^{+/-} and hAPP/*Tau*^{-/-} mice were less severe and occurred at longer latencies than in hAPP/*Tau*^{+/+} mice ($P < 0.01$; Fig. 4, A and B).

Tau reduction also increased resistance to PTZ in hAPP-nontransgenic mice, lowering seizure severity and delaying seizure onset ($P < 0.01$; Fig. 4, A and C). To confirm that tau reduction could reduce aberrant neuronal overexcitation, we challenged mice with excitotoxic doses of the glutamate receptor agonist kainate. As expected, intraperitoneal injection of kainate dose-dependently induced seizures in *Tau*^{+/+} mice (Fig. 4D). In contrast, *Tau*^{+/-} and *Tau*^{-/-} mice were resistant to kainate across a range of doses ($P < 0.05$; Fig. 4D). Thus, tau modulates sensitivity to excitotoxins and may be involved in regulating neuronal activity. The excitoprotective effect of tau reduction in mice without hAPP is more likely related to a physiological function of tau than to the removal of a pathological form of the protein. Sensitization of neurons to A β by physiological forms of tau could explain why

tau reduction is effective in hAPP/*Tau*^{+/+} mice despite their lack of obvious tau modifications.

Our findings raise the possibility that tau reduction could protect against AD and other neurological conditions associated with excitotoxicity. Of course, the therapeutic implications of our findings must be interpreted with caution. First, there are differences between the mouse model and AD, including the absence of substantial neuronal loss or neurofibrillary pathology in hAPP mice. The contribution of these abnormalities to AD-related cognitive impairment, relative to the role of reversible A β -induced neuronal dysfunction that is modeled in hAPP mice, remains to be determined (30). Second, microdeletions of chromosome 17q21 encompassing the tau gene are associated with learning disabilities in humans (31), although abnormalities in these individuals may relate to insufficiency of other genes in the region, such as the corticotropin-releasing hormone receptor gene, which is implicated in neuropsychiatric disease (32). We found no adverse effects of tau reduction on health or cognition in mice, and the evidence that even partial tau reduction robustly protected mice from A β and excitotoxic agents highlights its potential benefits.

Fig. 4. Tau reduction increased resistance to excitotoxin-induced seizures. (A) Tau reduction lowered seizure severity after a single intraperitoneal injection of PTZ (40 mg/kg; $n = 10$ to 11 mice per genotype; age 4 to 7 months; ANOVA: tau effect, $P < 0.0001$). Seizures were less severe in hAPP/*Tau*^{+/-} and hAPP/*Tau*^{-/-} mice than in hAPP/*Tau*^{+/+} mice (** $P < 0.01$ versus hAPP/*Tau*^{+/+}). Seizures were also less severe in *Tau*^{-/-} mice than in *Tau*^{+/+} mice (### $P < 0.01$ versus *Tau*^{+/+}). (B and C) Latency to reach each stage of seizure severity after PTZ administration. (B) PTZ-



induced seizures occurred more rapidly in hAPP/*Tau*^{+/+} mice than hAPP/*Tau*^{+/-} and hAPP/*Tau*^{-/-} mice (RMANOVA: $P < 0.01$). (C) Tau reduction also slowed the onset of PTZ-induced seizures in mice without hAPP (RMANOVA: $P < 0.001$). Error bars in (A) to (C) show SEM. (D) After a single intraperitoneal injection of kainate at the doses indicated, occurrence of generalized tonic-clonic seizures was scored. Tau reduction lowered susceptibility to kainate, shifting dose-response curves to the right ($n = 19$ to 24 mice per genotype; age 2 to 5 months; logistic regression: $P < 0.05$).

References and Notes

- R. Tanzi, L. Bertram, *Cell* **120**, 545 (2005).
- J. Lewis *et al.*, *Science* **293**, 1487 (2001).
- M. Rapoport, H. N. Dawson, L. I. Binder, M. P. Vitek, A. Ferreira, *Proc. Natl. Acad. Sci. U.S.A.* **99**, 6364 (2002).
- S. Oddo, L. Billings, J. P. Kesslak, D. H. Cribbs, F. M. LaFerla, *Neuron* **43**, 321 (2004).
- C. X. Gong, F. Liu, I. Grundke-Iqbal, K. Iqbal, *J. Neural Transm.* **112**, 813 (2005).
- K. Iqbal *et al.*, *Biochim. Biophys. Acta* **1739**, 198 (2005).
- W. H. Stoothoff, G. V. Johnson, *Biochim. Biophys. Acta* **1739**, 280 (2005).
- I. Khlistunova *et al.*, *J. Biol. Chem.* **281**, 1205 (2006).
- C. A. Dickey *et al.*, *FASEB J.* **20**, 753 (2006).
- A. J. Myers *et al.*, *Hum. Mol. Genet.* **14**, 2399 (2005).
- L. Mucke *et al.*, *J. Neurosci.* **20**, 4050 (2000).
- H. N. Dawson *et al.*, *J. Cell Sci.* **114**, 1179 (2001).
- Materials and methods are available as supporting material on Science Online.
- J. J. Palop *et al.*, *Proc. Natl. Acad. Sci. U.S.A.* **100**, 9572 (2003).
- D. T. Kobayashi, K. S. Chen, *Genes Brain Behav.* **4**, 173 (2005).
- O. Steward, J. Loesch, W. C. Horton, *Brain Res. Bull.* **2**, 41 (1977).
- K. K. Hsiao *et al.*, *Neuron* **15**, 1203 (1995).
- J. Chin *et al.*, *J. Neurosci.* **24**, 4692 (2004).
- S. Lesné *et al.*, *Nature* **440**, 352 (2006).
- E. Planet *et al.*, *J. Neurosci.* **24**, 2401 (2004).
- S. Y. Park, A. Ferreira, *J. Neurosci.* **25**, 5365 (2005).
- T. Liu *et al.*, *J. Neurochem.* **88**, 554 (2004).
- K. SantaCruz *et al.*, *Science* **309**, 476 (2005).
- R. B. Knowles *et al.*, *Proc. Natl. Acad. Sci. U.S.A.* **96**, 5274 (1999).
- J. W. Geddes *et al.*, *Science* **230**, 1179 (1985).
- M. P. Mattson, *Nature* **430**, 631 (2004).
- J. W. Olney, D. F. Wozniak, N. B. Farber, *Arch. Neurol.* **54**, 1234 (1997).
- J. C. Amatniek *et al.*, *Epilepsia* **47**, 867 (2006).
- R. A. Del Vecchio, L. H. Gold, S. J. Novick, G. Wong, L. A. Hyde, *Neurosci. Lett.* **367**, 164 (2004).
- J. J. Palop, J. Chin, L. Mucke, *Nature* **443**, 768 (2006).
- J. R. Lupski, *Nat. Genet.* **38**, 974 (2006).

32. F. Holsboer, *Curr. Opin. Investig. Drugs* 4, 46 (2003).
 33. We thank M. Vitek and H. Dawson for tau knockout mice; P. Seubert and P. Davies for antibodies; H. Solano, X. Wang, and Y. Zhou for technical assistance; C. McCullough for advice on statistics; D. McPherson and L. Manuntag for administrative support; and G. Howard and S. Ordway for editorial review. L.M. received

consulting fees from Merck and honoraria from Amgen, Elan, and Pfizer. E.D.R. received consulting fees from Rinat Neuroscience. Supported by NIH grants AG011385 and AG022074 (L.M.), MH070588 (K.S.L), and NS054811 (E.D.R.); the Giannini Foundation (E.D.R.); the S.D. Bechtel Jr. Young Investigator Award (E.D.R.); and the NIH National Center for Research Resources grant RR18928-01.

Supporting Online Material

www.sciencemag.org/cgi/content/full/316/5825/750/DC1
 Materials and Methods
 Figs. S1 to S7
 References

26 February 2007; accepted 27 March 2007
 10.1126/science.1141736

Regulation of NF- κ B Activation in T Cells via Association of the Adapter Proteins ADAP and CARMA1

Ricardo B. Medeiros,^{1*} Brandon J. Burbach,^{1*} Kristen L. Mueller,¹ Rupa Srivastava,¹ James J. Moon,² Sarah Highfill,¹ Erik J. Peterson,³ Yoji Shimizu^{1†}

The adapter protein ADAP regulates T lymphocyte adhesion and activation. We present evidence for a previously unrecognized function for ADAP in regulating T cell receptor (TCR)-mediated activation of the transcription factor NF- κ B. Stimulation of ADAP-deficient mouse T cells with antibodies to CD3 and CD28 resulted in impaired nuclear translocation of NF- κ B, a reduced DNA binding, and delayed degradation and decreased phosphorylation of I κ B (inhibitor of NF- κ B). TCR-stimulated assembly of the CARMA1-BCL-10-MALT1 complex was substantially impaired in the absence of ADAP. We further identified a region of ADAP that is required for association with the CARMA1 adapter and NF- κ B activation but is not required for ADAP-dependent regulation of adhesion. These findings provide new insights into ADAP function and the mechanism by which CARMA1 regulates NF- κ B activation in T cells.

Adapter proteins nucleate multimolecular complexes that are essential for effective transmission of intracellular signals during an adaptive immune response (1). In T lymphocytes, the adhesion- and degranulation-promoting adapter protein (ADAP) regulates T cell receptor (TCR)-dependent changes in the function of integrin adhesion receptors (2, 3). ADAP-deficient (ADAP^{-/-}) T cells also exhibit impaired proliferation and cytokine production after stimulation of the TCR and the CD28 costimulatory receptor (2, 3). Stimulation of these receptors leads to activation of the NF- κ B family of transcription factors, which are critical for T cell activation and survival (4). A multiprotein complex consisting of the membrane-associated adapter protein CARMA1 (5, 6), the caspase-like protein MALT1 (7, 8), and the adapter protein BCL-10 (9) is critical for TCR-dependent activation of the I κ B kinase complex and subsequent NF- κ B nuclear translocation (10).

Like ADAP-deficient T cells, protein kinase C θ (PKC θ)-deficient T cells exhibit defective TCR-mediated proliferation, even though proximal TCR signaling events, such as extracellu-

lar signal-regulated kinase (ERK) activation, are normal (11). Therefore, we examined PKC θ -dependent signaling in ADAP^{-/-} T cells (12).

Membrane localization of PKC θ was similar in ADAP^{+/-} and ADAP^{-/-} T cells upon stimulation with antibodies to CD3 and CD28 (Fig. 1, A and B). Stimulated ADAP^{+/-} and ADAP^{-/-} T cells also showed similar levels of PKC θ phosphorylation (Fig. 1C). Thus, ADAP is not required for TCR signaling events leading to and including PKC θ activation. Because PKC θ regulates NF- κ B activation downstream of the TCR (11, 13), we next examined NF- κ B signaling in ADAP^{-/-} T cells. Image scanning flow cytometry (14, 15) (fig. S1) revealed a striking defect in p65 nuclear translocation after stimulation of ADAP^{-/-} lymph node T cells (Fig. 2, A and B) or CD4 T cells (fig. S2) by CD3 and CD28 (CD3/CD28). In contrast, no impairment in NF- κ B activation was detected after stimulation with tumor necrosis factor- α (TNF- α), which activates NF- κ B independently of the TCR. These results were confirmed with electrophoretic mobility shift assays (Fig. 2C). ADAP^{-/-} T cells also displayed defective NF- κ B translocation after treatment with phorbol 12-myristate 13-acetate (PMA), which activates PKC (Fig. 2, A and B).

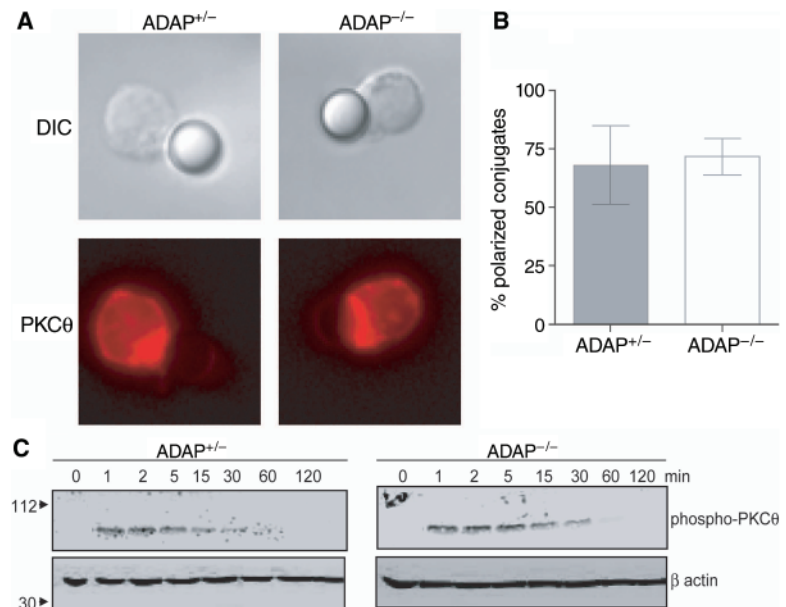


Fig. 1. TCR-dependent membrane localization and activation of PKC θ in ADAP^{-/-} T cells. (A) Localization of PKC θ (bottom) in ADAP^{+/-} and ADAP^{-/-} T cells to the contact site with beads coated with antibodies to CD3 and CD28. Differential interference contrast (DIC) images are shown in top panels. (B) Quantification of PKC θ localization. T cell-bead conjugates (minimum 90 per group) were scored for PKC θ polarization from two independent experiments. Graph shows the average percent of T cell-bead conjugates with polarized PKC θ (\pm SD). (C) Phosphorylation of PKC θ after CD3/CD28 stimulation of ADAP^{+/-} and ADAP^{-/-} T cells for the indicated time points was assessed by Western blotting of whole-cell lysates with antibody to phosphorylated PKC θ (Thr⁵³⁸) (top panels). Blots were also probed with antibody to β -actin (bottom panels).

¹Department of Laboratory Medicine and Pathology, Center for Immunology, Cancer Center, University of Minnesota Medical School, Minneapolis, MN 55455, USA. ²Department of Microbiology, Center for Immunology, University of Minnesota Medical School, Minneapolis, MN 55455, USA. ³Department of Medicine, Center for Immunology, Cancer Center, University of Minnesota Medical School, Minneapolis, MN 55455, USA.

*These authors contributed equally to this work.

†To whom correspondence should be addressed. E-mail: shimi002@umn.edu